Cancer Treatment and Research Communications 29 (2021) 100467

Contents lists available at ScienceDirect

Cancer Treatment and Research Communications

journal homepage: www.sciencedirect.com/journal/cancer-treatment-and-research-communications

Discovery of a novel anti PD-L1 X TIGIT bispecific antibody for the treatment of solid tumors.

Yang Xiao [a,*], Peiran Chen [a,b], Cheng Luo [a], Ziyang Xu [a,c], Xue Li [a], Liqiong Liu [a], Liwen Zhao [a]

[a] Nanjing Sanhome Pharmaceutical Co., Ltd., Nanjing 221116, China
[b] China Pharmaceutical University, Nanjing 211198, China
[c] Nanjing University, Nanjing 210046, China

ARTICLE INFO

Keywords:
Bispecific antibody
PD-1/PD-L1
TIGIT
Cancer immunotherapy

ABSTRACT

The emergence of immune checkpoint inhibitors (ICIs), mainly based on PD-1/PD-L1 blockade has revolutionized the therapeutic landscape of cancer. Despite the huge clinical success ICIs have achieved, about 70% of patients still showed de novo and adaptive resistance. Exploring novel and complementary immune checkpoint molecules in addition to PD-1/PD-L1 is in great urgency. *T* cell immunoglobulin and ITIM domain (TIGIT) is a co-inhibitory molecule containing an immunoreceptor tyrosine-based inhibition motif (ITIM) within its cytoplasmic tail, and is highly expressed on regulatory *T* cells and activated CD4+ *T*, CD8+ *T*, and NK cells. We generated a novel single chain Fab heterodimeric bispecific IgG antibody format targeting PD-L1 and TIGIT with one binding site for each target antigen. The bispecifc antibody BiAb-1 is based on "knob-into-hole" technology for heavy chain heterodimerization with a glycine serine linker connecting the 3′ end of Cκand the 5′ end of VH to prevent wrong pairing of light chains. BiAb-1 was produced with high expression yields and show simultaneous binding to PD-L1 and TIGIT with high affinity. Importantly, cytokine production was enhanced by BiAb-1 from staphylococcal enterotoxin B (SEB) stimulated PBMCs. BiAb-1 also demonstrated potent anti-tumor efficacy in multiple tumor models and superior activity to PD-1/PD-L1 blockade molecules. In conclusion, we have applied rational antibody engineering technology to develop a monovalent heterodimeric bispecifc antibody, which combines the blockade of both PD-1/PD-L1 and TIGIT/CD155 pathways simultaneously and results in superior anti-tumor efficacy in multiple tumor models over existing anti PD-1/PD-L1 molecules.

Introduction

The use of immune checkpoint inhibitors (ICIs) has become the treatment paradigm for multiple cancer types in the last decade. Starting from the initial approval Ipilimumab in 2011, anti-PD-1/PD-L1 agents are now a routinely used treatment option for more than 20 different indications. Although responses to ICIs can last year's even without continuous treatment [1–7], the vast majority of patients do not experience clinical benefits from ICIs. The response rate to single-agent PD-1/PD-L1 blockade in most cancers is limited to 10%—25% [3, 8–10] except melanoma, Merkel cell lymphoma and MSI-high tumors. Furthermore, disease progression can still happen among patients who initially respond to ICIs.

Resistance to ICIs can be classified to several categories including neoantigen lost, lack of *T* cell priming, defects in IFN-γ signaling etc. One hot research area is the present of additional check point inhibitor molecule [5, 11, 12]. *T*-cell Ig and ITIM domain (TIGIT) interact with CD155 (PVR) is considered as an alternative pathway exists in addition to the "classical" co-inhibitory PD-1/PD-L1 pathway. CD155 showed virtually no correlation to PD-L1 in its expression pattern across lung adenocarcinoma patients[13] and coblock TIGIT/CD155 and PD-1/PD-L1 pathways have shown synergistic effects both in mouse tumor model and clinical trials[14, 15]. However, to our knowledge most researches of TIGIT/CD155 and PD-1/PD-L1 pathways coblockade are based on the combinatorial use of two separated antibody molecules. It would be interesting to see coblocking TIGIT/CD155 and PD-1/PD-L1 pathways together as one molecule could have synergistic tumor eliminating effects.

In the past, scFab antibodies were mostly expressed in bacterial and yeasts and were used in phage display [16]. Here, we developed a novel scFab antibody format targeting both PD-L1 and TIGIT with high affinity and combines robust expression and overcomes the light chain miss

* Corresponding author at: Nanjing Sanhome Pharmaceutical Co., Ltd., No.99 Yunlianghexi Road, Xuanwu district Nanjing, Jiangsu Province R.P. China 210007.
E-mail address: xy19860613@163.com (Y. Xiao).

https://doi.org/10.1016/j.ctarc.2021.100467

Available online 27 September 2021

Table 1
Biochemical characteristics of HuPLxx-1 against hPD-L1.

	ELISA based activity		Cell based activity		Binding (BLI)		
	EC_{50} (nM)	IC_{50} (nM)	EC_{50} (nM)	IC_{50} (nM)	K_{on} (1/Msec)	K_{off} (1/*sec*)	K_D (nM)
HuPLxx-1	0.053	5.37	0.88	7.85	1.49E-09	1.85E + 05	2.76E - 04
Ate	0.019	4.37	0.73	7.49			

Definitions:.
K_{on} = Biacore association rate; K_{off} = Biacore dissociation rate; K_D = Biacore binding affinity.

Table 2
Biochemical characteristics of HuTyy-1 against hTIGIT.

	ELISA based activity		Cell based activity		Binding (BLI)		
	EC_{50} (nM)	IC_{50} (nM)	EC_{50} (nM)	IC_{50} (nM)	K_{on} (1/Msec)	K_{off} (1/*sec*)	K_D (nM)
HuTyy-1	2.43	1.02	0.20	1.40	2.43E - 09	7.92E + 05	1.92E - 03
22G2	1.91	1.34	0.41	1.67			

pairing issue of bispecific heterodimeric IgG antibodies [17]. Furthermore, we compared the anti-tumor effect of PD-1/PD-L1 blockade molecules and the bispecific antibody in vivo in two different models. The bispecifc antibody demonstrates superior anti-tumor effect over single agent and may present a potential strategy to for clinical usage.

Materials and methods

Cell lines, animals and reagents

The human tumor cell lines HEK293E, HCC827 and mouse CHO-K1 were purchased from ATCC, and maintained in RPMI 1640 containing 10% fetal bovine (FBS). MC38-hPD-L1 and Raji-hPD-L1 were constructed and purchased from Biocytogen, and maintained in Dulbecco's Modified Eagle's medium (Biocytogen) containing 10% FBS. ExpiCHO-S™ and Sp2/0 were purchased from Thermol Fisher Scientific and cultured as instructed. CHO-K1-hPD-L1, CHO-K1-hTIGIT were subcloned after stably transducing with the plasmid contained full-length sequence of human PD-L1 or human TIGIT. About 4 – 6-week-old female Balb/c, SJL, NOD.*Cg-Prkdc*^{scid}*Il2rg*^{tm1Wjl}/SzJ (NSG) and B-hPD-L1/hTIGIT mice were purchased from Biocytogen (Beijing, China). PE-conjugated anti-human Fc antibody and PE Goat anti-mouse Fc antibody were purchased from Biolegend. Isotype IgG4 was purchased from CrownBio. Anti-PD-L1 antibody sequence (Atezolizumab) was synthesized according to patent (patent no.: US 8217,149). Anti-TIGIT antibody (22G2) sequence was synthesized according to patent (patent no.: US20160176963A1). Proteins like TIGIT-his, TIGIT-mfc, PD-1/L1-his and PD-1/L1-mfc were produced by our laboratory.

BLI assays

BLI measurements were performed with ForteBio Octet RED96 instruments and ForteBio biosensors to determine the equilibrium binding constant (K_D) of BiAb-1. In brief, Anti-hTIGIT or anti-hPD-L1 was immobilized on CM5 chip. The gradient diluted BiAb-1 was injected at a constant flow rate. The equilibrium dissociation constant K_D (Kd/Ka) was calculated by using the ForteBio Octet RED96 software.

Cell-based binding and blocking assays

1.5×10^6 CHO-K1-hPD-L1 or CHO-K1-hTIGIT cells per well was incubated with increasing amounts of BiAb-1 or indicated antibody for 40 min at 4 °C. After incubation, samples were washed by PBS for 3 times and stained with PE-conjugated anti-human Fc antibody in dark for 40 min at room temperature, then analyzed by flow cytometer (ACEABIO, Novocyte). The PD-L1 and TIGIT blocking activity of BiAb-1 were evaluated according to the previous report [18]. Briefly, PD-L1-mfc or TIGIT-mfc were incubated with a series dilution of BiAb-1 or Isotype IgG4 on ice for 30 min respectively, followed by incubation with detection antibody PE Goat anti-mouse Fc antibody. Cells were then washed with FACS buffer to remove the unbound fluorescent antibodies. Data was acquired on a flow cytometer (ACEABIO, Novocyte) and analyzed by FlowJo.

Human PBMC activation assays

Human PBMCs, which were purified from whole human blood of healthy donors by using EasySep™ (STEMCELL Technologies), were seeded at 1×10^5 per well in a 96-well plate, serial diluted proteins or IgG4 isotype were added l in 96-well plate. 100 ng/ml staphylococcal enterotoxin B (SEB; S4881, Sigma-Aldrich) were added to the plate, following co-incubation for 72 h at 37 °C. The IL-2 or IFN-γ release in the supernatant was determined, following human IL-2 or IFN-γDuoSet kit instructions (R&D systems).

Humanization of antibodies

Humanization of mouse anti-PD-L1 or anti-TIGIT variable regions was performed using a CDR-graft strategy as described previously [19]. Briefly, cDNAs containing human acceptor framework, VH1–18 for αPD-L1 heavy chain and VK4–1 for αPD-L1 light chain, VH3–7 for αTIGIT heavy chain and VK1–17 for αTIGIT light chain, with anti-PD-L1 or anti-TIGIT CDR donor sequences were synthesized in vectors containing either human IgG4 constant region for the heavy chain, or human kappa constant region for the light chain. To recover binding activity, back-mutations to mouse sequence in the framework regions of both the VH and VL domains were introduced. Proteins were expressed and purified as IgG, then assessed for binding or blocking activity by FACS, and human PBMC activation assay as described above.

Human cancer cell line xenograft tumor model

HCC827 or Raji-hPD-L1 tumor cells were subcutaneously implanted into the flanks of female NSG mice. When tumors reached volumes of ~100 mm^3, 1×10^7 freshly isolated PBMCs were administered intravenously (IV) and mice were treated with indicated proteins or human IgG4 at 20 mg/kg twice a week for a total of three weeks. Tumor measurements were collected using Vernier caliper, and volumes were calculated by use of the modified ellipsoid formula ½ x length x width [2]. All animals were housed in a pathogen-free environment and were treated following the standards of Pharmaceutical Animal Center of China Pharmaceutical University

Mouse syngeneic tumor model

B-hPD-L1/hTIGIT mice were purchased from Biocytogen. MC38-hPD-L1 tumor cells were subcutaneously implanted into the flanks of female B-hPD-L1/hTIGIT mice. When tumors reached volumes of ~100 mm^3, mice were treated with indicated proteins or human IgG4 at 3 mg/kg or 6 mg/kg twice a week for a total of 3weeks. Tumor measurements were collected using Vernier caliper, and volumes were calculated by use of the modified ellipsoid formula ½ x length x width [2].

Statistical analysis

Means, SDs, nonlinear analysis to determine EC_{50} and IC_{50} values were calculated by GraphPad Prism (version 6.02).

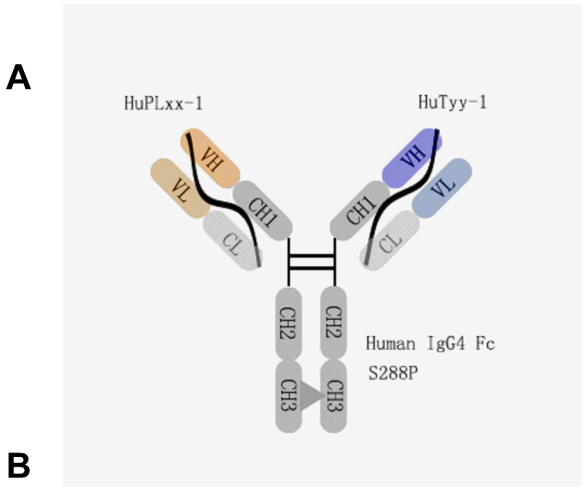

Fig. 1. Design of BiAb-1 bispecific antibodies. (A) Schematic diagram of BiAb-1. VH and VL domains in the bispecific antibody are derived from the parental antibodies HuTyy-1 (TIGIT; brown) and HuPLxx-1 (PD-L1; blue). Dimerization of the two different heavy chains in BiAb-1 was facilitated by the knob-into-hole mutations (gray triangle) in the CH3 domain. (B) Analytical SEC was used to estimate the presence of aggregates in the BiAb-1 molecule after protein A, AEX and CHT purification. (C) MS analysis confirmed sequence integrity of BiAb-1, and no by-products, such as hole-hole dimers, knob-knob dimers, half-antibodies were detectable.

Results

Generation and selection of parental antibodies

Both PD-L1 and TIGIT parental antibodies were generated by repeated immunization of mice with purified antigen or stably transfected CHO-K1 cells. Antibody producing B cells were harvested from spleens and draining lymph nodes and fused with mouse myeloma cells to generate hybridomas. We generated more than 150 different antibodies for each target and screened these antibodies by protein-based binding, cell-based binding and human PBMC activation assays. Clone PLxx and Tyy were selected based on these tests. The two

Table 3
Biochemical characteristics of BiAb-1.

	Cell based activity		ELISA based activity		Binding (BLI)		
	EC_{50} (nM)	IC_{50} (nM)	EC_{50} (nM) (Human)	EC_{50} (nM) (*Cynomolgus*)	K_{on} (1/Msec)	K_{off} (1/*sec*)	K_D (nM)
BiAb-1	0.58	3.19	0.73	0.092	1.32E - 09	2.07E + 05	2.73E - 04
Ate	1.77	1.68					
	Cell based activity		ELISA based activity		Binding (BLI)		
	EC_{50} (nM)	IC_{50} (nM)	EC_{50} (nM) (Human)	EC_{50} (nM) (Cynomolgus)	K_{on} (1/Msec)	K_{off} (1/*sec*)	K_D (nM)
BiAb-1	1.30	4.08	4.96	0.61	3.06E - 09	1.09E + 06	3.33E - 03
22G2	0.39	2.17					

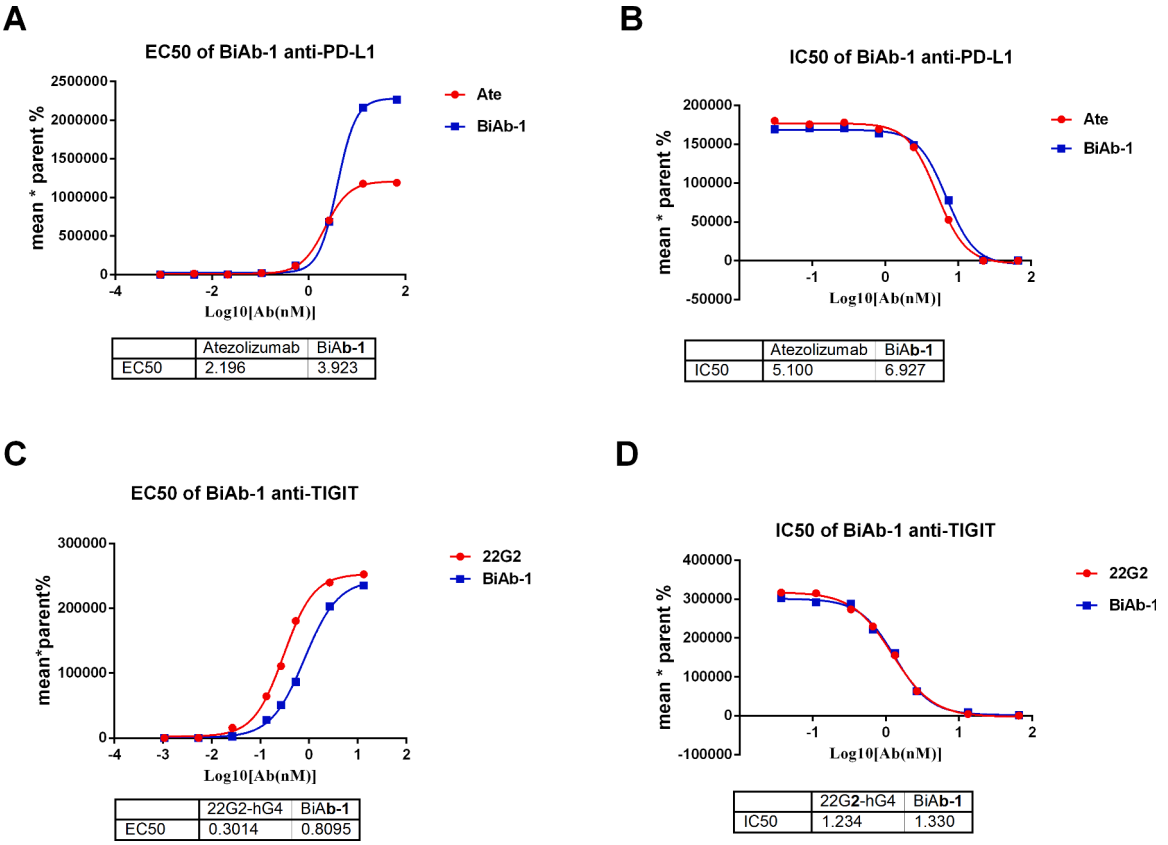

Fig. 2. Characterization of BiAb-1. (A-D)The binding and blocking activity of BiAb-1 – CHO-K1 cell lines (CHO-K1-hPD-L1 or CHO-K1-hTIGIT) was evaluated by flow cytometry, Atezolizumab and 22G2 were set as a positive control respectively.

antibodies sequence were further humanized and characterized in biochemical and whole cell binding and blocking assays to determine affinity, cell based activity and cross-reactivity as described above. HuPLxx-1 bound to human PD-L1 with EC_{50} values of 0.053 nM. The affinity of HuPLxx-1 to human PD-L1 was measured by Fortebio and the K_D value is 1.49E-09. HuPLxx-1 bound to human PD-L1 expressing CHO-K1 cells with an EC_{50} value of 0.88 nM. HuPLxx-1 was measured for its capacity to block PD-1 and PD-L1 interaction using a competitive FACS assay. The IC_{50} of HuPLxx-1 was 7.85 nM, which is comparable with Atezolizumab (Table 1). HuTyy-1 bound to human TIGIT with EC_{50} values of 2.43 nM. The affinity of HuTyy-1 to human TIGIT was measured by Fortebio and the K_D value is 2.43E-09. HuTyy-1 bound to human TIGIT expressing CHO-K1 cells with an EC_{50} value of 0.2 nM. HuTyy-1 was measured for its capacity to block TIGIT and PVR interaction using a competitive FACS assay. The IC_{50} of HuTyy-1 was 1.4 nM, which is comparable with 22G2 (Table 2).

Generation of a heterodimeric scFab bispecific antibody targeting PD-L1 and TIGIT

The bispecific antibody was designed and generated based on a human IgG4 isotype with heavy chains composed of a variable VH domain and three constant domains CH1, CH2, CH3. The corresponding light chains are composed of a variable VL domain and a constant Cκ domain. BiAb-1 was assembled with an PD-L1 binding arm composed of a single-chain fab fragment of HuPLxx-1 with the light chain attached to the N terminus of the VH domain by a $(GGGGS)_8$ linker while an TIGIT binding arm composed of a single-chain fab fragment of HuTyy-1 with the light chain attached to the N terminus of the VH domain by a $(GGGGS)_8$ linker to form the second heavy chain (Fig. 1A). Heterodimerization of the two heavy chains was achieved by application of the knobs-into-hole technology [20]. The knob mutation (T366W) was introduced into the CH3 domain of the scFab HuTyy-1 heavy chain, and three mutations to form a hole (T366S, L368A, and Y407V) were introduced into the CH3 domain of the scFab heavy chain of HuPLxx-1. In addition, two cysteine residues were introduced (S354C on the knob and Y349C on the hole side) to form a stabilizing disulfide bond between

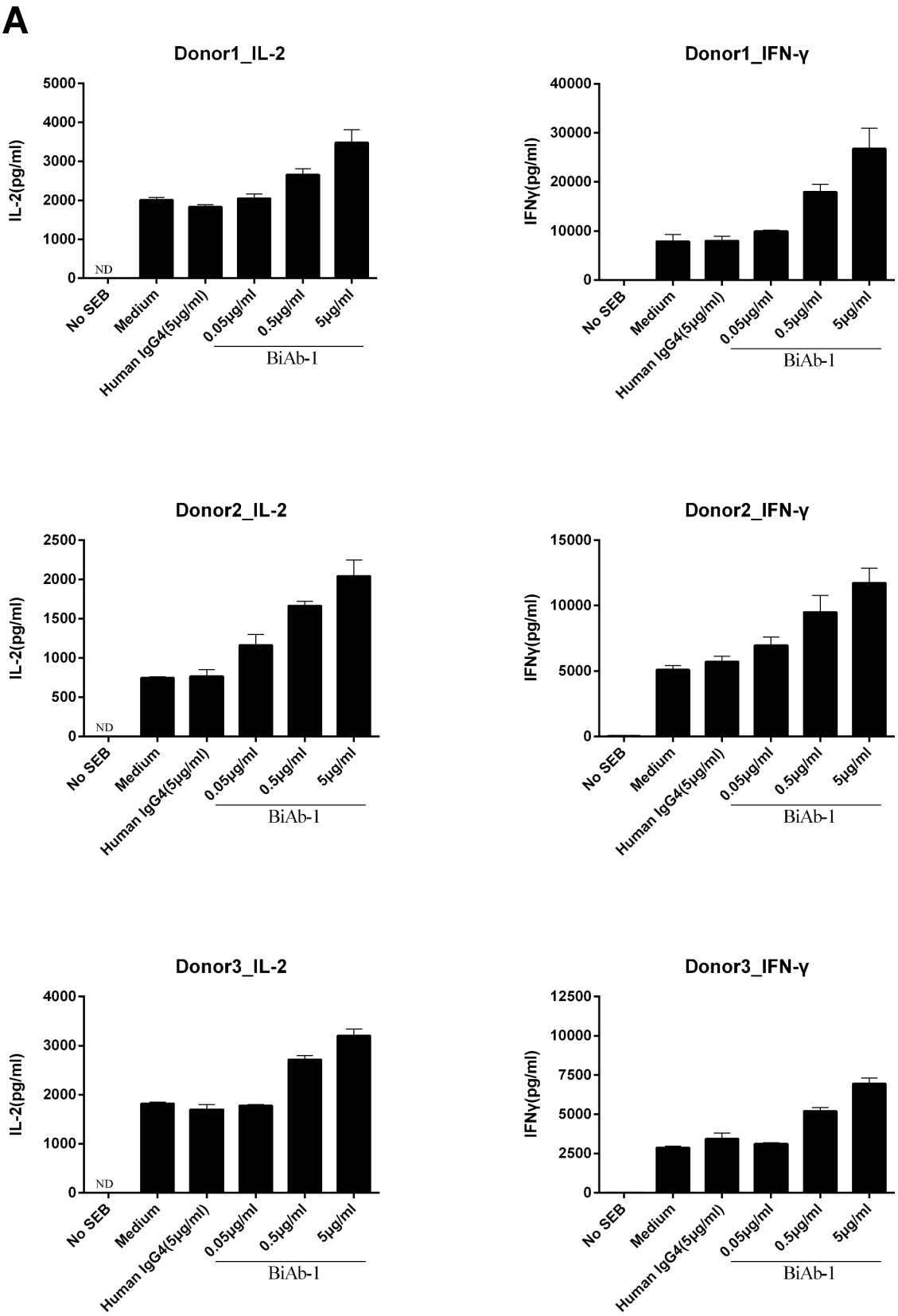

Fig. 3. In vitro activation of human PBMCs. PBMCs were extracted from three healthy donors. Supernatants were measured for IL-2 and IFN-γ production by ELISA. Each data point represents the average of 3 replicates, with error bars representing the SEM.

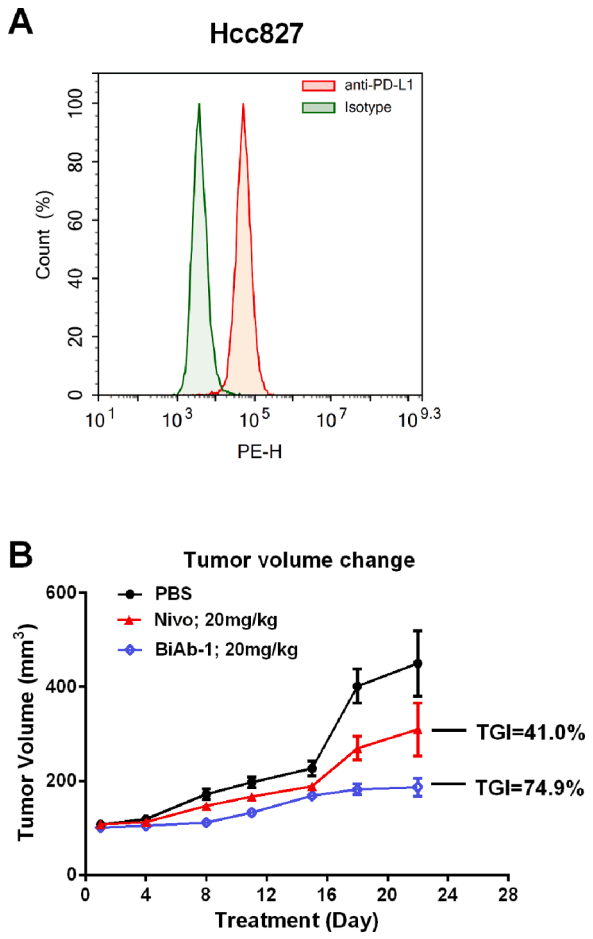

Fig. 4. Anti-tumor effect of BiAb-1 in HCC827 xenograft model. (A) Human PD-L1 expression levels of HCC827 cells was evaluated by flow cytometry. (B) The NSG mice were implanted HCC827 cells subcutaneously until tumor volumes reached approximately 100 mm [3]. After received human PBMCs by intraperitoneal injection, the mice were treated with the indicated doses of antibodies or vehicle via intraperitoneal administration twice a week. Tumor volumes are plotted as means with SD ($n = 6$).

the heterodimeric heavy chains. Further mutations including S228P was introduced to stabilize the IgG molecule.

Generation of stable CHO cell lines

Most therapeutic antibodies in clinical development are currently produced in stable CHO cell lines. Therefore, the manufacturing scalability of BiAb-1 was evaluated in CHO cells. HuTyy-1 scFab knob heavy and light chain and HuPLxx-1 scFab hole heavy and light chain were condon optimized and constructed two separate expression plasmids and overexpressed in CHO-K1Q cells (Quacell Biotechnology) using a glutamine synthase expression system. A total number of 567 clones were analyzed for IgG titers, and 59 clones were selected for generic fed batch productions. Clone 16 was selected with yields of 2.5~3.2 g/l and a purity of 75% after one step Protein A purification. The relative heterodimer rate was >95%, determined by MS (Fig. 1C).

Biochemical characteristics of bispecific antibody BiAb-1

The bispecifc antibody BiAb-1 was analyzed for affinity and cell-based activity using BLI analysis and whole cell binding and blocking assays as described above. BiAb-1 maintained the high affinity and cell-based activity of its parental antibodies (Table 3) with the exception of cell-based PD-L1 binding, BiAb-1 shows significantly higher average fluorescence intensity upon binding to CHO-K1-PD-L1 cells, probably due to more molecules binding to the targets (Fig. 2A–D).

In vitro activation of human PBMCs

SEB stimulated PBMCs were used to study the functional consequences of PDL1 and TIGIT co-neutralization in vitro. Frozen stored PBMCs were recovered by centrifuge and stimulated with 100 ng/ml SEB and cultured with indicated proteins for 72 h. As showed in Fig. 3, BiAb-1 significantly enhanced the IL-2 and IFN-γ production in a dose dependent manner in three different donors.

Anti-Tumor effect of BiAb-1 in HCC827 xenograft model

To assess BiAb-1 activity in vivo, NSG mice were implanted subcutaneously with the human NSCLC cell line HCC827, which showed high PD-L1 and PVR expression (Fig. 4A) and engrafted with freshly isolated human PBMCs. The mice were then dosed i.p, twice weekly, with either isotype or proteins indicated at 20 mg/kg per dose. After three weeks of dosing, both Nivolumab and BiAb-1 treatment groups displayed significantly inhibited tumor growth compared to control group (Fig. 4B). BiAb-1 also displayed significant enhanced anti-tumor effect compared with Nivolumab. These results indicated that combine PD-L1 and TIGIT blockade together significantly enhanced anti-tumor responses.

Anti-Tumor effect of BiAb-1 in Raji-hPD-L1 xenograft model

To assess BiAb-1 activity in vivo, NSG mice were implanted subcutaneously with the human lymphoma cell line Raji stably transfected with PD-L1 expression (Fig. 5A) and engrafted with freshly isolated human PBMCs. The mice were then dosed i.p., twice weekly, with either isotype or proteins indicated at 20 mg/kg per dose. After three weeks of dosing, Atezolizumab, HuPLxx-1 and HuTyy-1 combination and BiAb-1 treatment groups displayed significantly inhibited tumor growth compared to control group (Fig. 5B). BiAb-1 also displayed enhanced anti-tumor effect compared with parental mabs combination. These results indicated that BiAb-1 may have novel mechanisms of action that are impossible to attain with combinations.

Anti-tumor effect of BiAb-1 in mouse MC38 syngeneic model

To further study the anti-tumor effect of BiAb-1 in a more relevant and translational approach, B-hPD-L1/hTIGIT mice were implanted subcutaneously with the mouse colorectal cancer cell line MC38-hPD-L1 and treated as described above. After four weeks of dosing, both Atezolizumab and BiAb-1 treatment groups displayed significantly inhibited tumor growth compared to control group (Fig. 6). The two doses of 3 mg/kg and 6 mg/kg BiAb-1 groups achieved 30.6% and 50.7% tumor growth inhibition (TGI), respectively, whereas 3 mg/kg Atezolizumab group achieved 35.6% TGI. In this study, BiAb-1 showed a dose-dependent and significant versus control group ($p < 0.05$) anti-tumor manner.

Discussion

Immune checkpoint inhibitors (ICIs) showed great benefit for responders. However, currently marketed anti-PD-1/PD-L1 agents have limited response rate over a variety of solid tumors as a single agent. Although combining anti-PD-1 mab and anti-CTLA4 mab significantly increased objective response rates in several indications, it also leads to increased severe adverse events (SAEs) [20–24]. Exploring additional safe and compensatory to PD-1/PD-L1 immune checkpoint molecules become necessary for unmet clinical needs.

We have constructed a novel heterodimeric scFab bispecific antibody that is capable of simultaneously binding PD-L1 and TIGIT and inducing potent cytokine expression in human PBMCs. The introduction of scFab

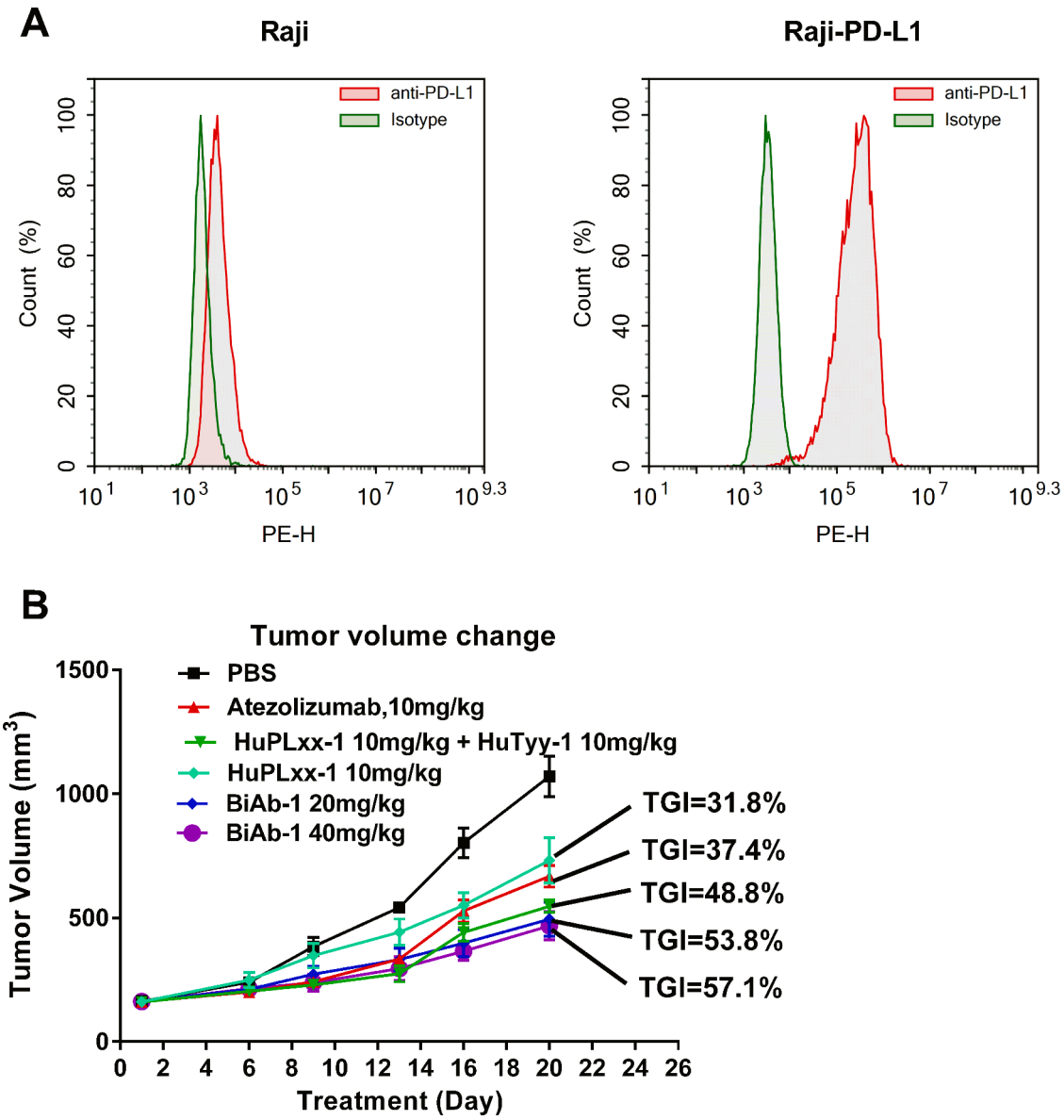

Fig. 5. Anti-tumor effect of BiAb-1 in Raji-hPD-L1 xenograft model. (A) Human PD-L1 expression levels of Raji cells versus Raji-hPD-L1 cells evaluated by flow cytometry. (B) The NSG mice were implanted Raji-hPD-L1 cells subcutaneously until tumor volumes reached approximately 100 mm [3]. After received human PBMCs by intraperitoneal injection, the mice were treated with the indicated doses of antibodies or vehicle via intraperitoneal administration twice a week. Tumor volumes are plotted as means with SD ($n = 6$).

arm allowed us to rapidly generate a bispecific antibody without the risk of large amount of aggregates usually happened to tetravalent scFv format and time or labor intensive optimization to find a common light chain. Here, we combined scFab technology and knob-into-hole heterodimerization of two distinct heavy chains to generate a novel bispecific antibody with good yields of ≥3 g/L with low amount of aggregates.

Potent in vivo efficacy of BiAb-1 was shown in two different mouse models. BiAb-1 led to almost complete tumor growth arrest in the PD-L1 positive human HCC827 cell line PBMC engraftment model and a significant tumor inhibition of B-hPD-L1/hTIGIT mouse MC38 syngeneic model. To our knowledge, this is the first PD-L1/TIGIT bispecific antibody reported to date. Further studies need to be carried out to investigate the differences of anti-tumor activity between PD-1/TIGIT and PD-L1/TIGIT bispecifc antibodies, whether the avidity binding of αPD-1 and αTIGIT single arms could navigate bisepcific molecules to PD-1+/TIGIT+ *T* cells, a more exhausted type of *T* cells in tumor microenvironment. It is also reported that the efficacy of anti-TIGIT mabs is dependent on functional FcγRs[25],[26], it would be worth investigating on whether WT IgG1 could increase the efficacy of BiAb-1.

Opdivo and Yervoy combo is the most successful IO combo to date and FDA has approved its usage for advanced melanoma, advanced renal cell carcinoma, metastatic non-small cell lung cancer, hepatocellular carcinoma and most recently malignant pleural mesothelioma. Despite the superior efficacy of the combo, it also increase the incidence of adverse events. Take the results of Checkmate 067 as an example, more grade 3 or 4 treatment-related adverse events or serious adverse events were reported with nivolumab plus ipilimumab than with nivolumab alone (59%vs 21% [27])and most importantly, the rate of diarrhea and colitis increased significantly (9%vs 3% for diarrhea and 8%vs 1% for colitis). Since gastrointestinal adverse events are signature AEs for CTLA4 and there are unmet clinical needs for patients with IBD or other potential autoimmune diseases that may not be suitable for PD-1 and CTLA4 combo, it is important to discover new IO targets. TIGIT is one of the safer IO targets thatshow promising preliminary efficacy results in the clinical stage. In phase II CITYSCAPE study, Tiragolumab in combination with Tecentriq showed an improvement in the overall

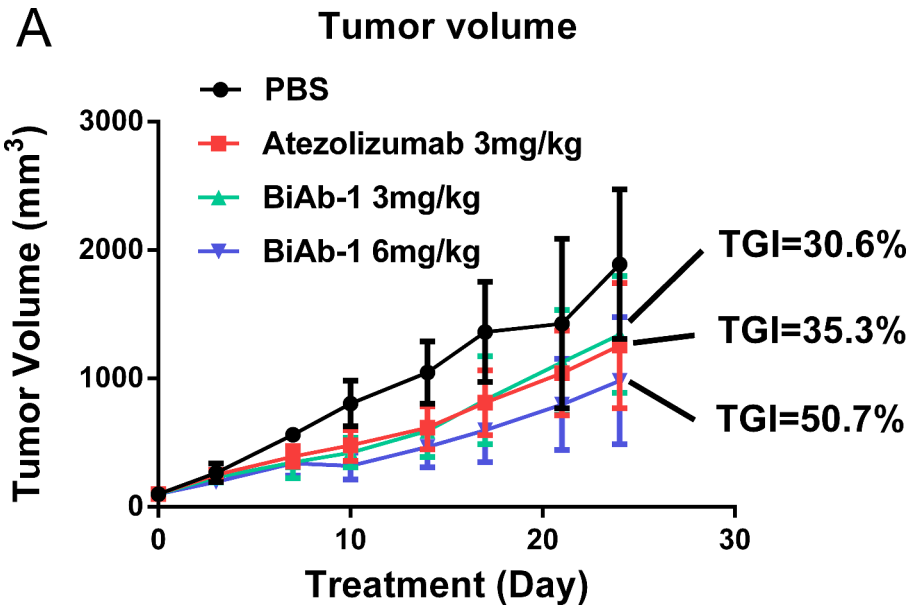

Fig. 6. Anti-tumor effect of BiAb-1 in mouse MC38 syngeneic model. B-hPD-L1/hTIGIT mice were implanted MC38-hPD-L1 cells subcutaneously. After the tumor volumes reached ~100 mm [3], the mice were prescribed indicated doses of antibodies or vehicle by intraperitoneal injection twice a week. Tumor volumes are plotted as means with SD ($n = 8$).

response rate (ORR; 37%vs. 21% with Tecentriq alone) and a 42% reduction in the risk of disease worsening or death (progression free survival; PFS) compared with Tecentriq alone, while having similar rates of all Grade 3 or more all-cause adverse events when combining the two immunotherapies compared with Tecentriq alone (48%vs. 44%). Moreover, MSD presented new data of Vibostolimab and Keytruda combo in ESMO 2020, among patients whose tumors express PD-L1 (tumor proportion score [TPS] ≥ 1%), the ORR was 46% and median PFS was 8.4 months, which is a significant improvement thanKeytruda alone historically, while having Grade 3–5 TRAEs occurred in 15% of the patients, which is about the same as Keytruda alone historically. Overall, TIGIT maybe a new IO target which could significantly improve the efficacy of PD-1/PD-L1 blockers while adding minimal toxicity.There are lots of preclinical studies on how the overexpression of PVRIG could dampen immune suppressive state and the disruption of PD-1/PD-L1 and TIGIT/PVRIG pathways together could reinvigorate the immune system [28], [29].The biomarkers for anti-PD-L1/TIGIT bispecific antibodychoice is rather straightforwardinhot tumors like NSCLC,Roche and MSD have both presented better results of PD-1/PD-L1 and TIGIT combotogether thanPD-1/PD-L1 blocker alone in preliminary clinical results.The problem becomes more complicated in cold tumors. Taking CRC as an example, although PVRIG has a relative high expression in CRC patients (data from human protein atlas website), one would imagine the efficacy of bispecific antibody would be limited in MSS CRC patients even if they have high PVRIG expression due to the lack of *T* cell infiltration. Novel biomarkers such as CD8+*T* cell density, tumor mutational burdenand neoantigen load would be moreidealforcertain tumor types.

In summary, our data demonstrates simultaneously blocking PD-1/PD-L1 and TIGIT/CD155 signaling pathways with one molecule could significantly increase the anti-tumor activity compared with single agent PD-1/PD-L1 agents. Therefore, BiAb-1 may be a promising new therapeutic option for the treatment of PD-L1+ tumors.

Ethical approval statement

The PBMCs were extracted from healthy donors, and the informed consent was obtained from them. All animal experiments in this research comply with the ARRIVE guidelines and were carried out in accordance with the National Institute of Health guide for the care and use of laboratory animals. All animals used in this experiment are female.

Formating of funding sources

This research did not receive any specific grant from funding agencies in the public, commercial, or not-for-profit sectors.

CRediT authorship contribution statement

Yang Xiao: Conceptualization, Formal analysis, Data curation, Writing – review & editing. **Peiran Chen:** Conceptualization, Formal analysis, Data curation, Writing – review & editing. **Cheng Luo:** Conceptualization, Formal analysis, Data curation, Writing – review & editing. **Ziyang Xu:** Conceptualization, Formal analysis, Data curation, Writing – review & editing. **Xue Li:** Conceptualization, Formal analysis, Data curation, Writing – review & editing. **Liqiong Liu:** Conceptualization, Formal analysis, Data curation, Writing – review & editing. **Liwen Zhao:** Conceptualization, Formal analysis, Data curation, Writing – review & editing.

Declaration of Competing Interest

The authors declare that they have no known competing financial interests or personal relationships that could have appeared to influence the work reported in this paper.

Acknowledgments

We thank Mixue Bai for FACS support and Xiaoli Sun for mass spectrometry technical assistance and data analysis.

References

[1] S.J. Antonia, H. Borghaei, S.S. Ramalingam, L. Horn, J. De Castro Carpeño, A. Pluzanski, M.A. Burgio, M. Garassino, L.Q.M. Chow, S. Gettinger, L. Crinò, D. Planchard, C. Butts, A. Drilon, J. Wojcik-Tomaszewska, G.A. Otterson, S. Agrawal, A. Li, J.R. Penrod, J. Brahmer, Four-year survival with nivolumab in patients with previously treated advanced non-small-cell lung cancer: a pooled analysis, Lancet Oncol. 20 (2019) 1395–1408.

[2] A. Bernard-Tessier, C. Baldini, P. Martin, S. Champiat, A. Hollebecque, S. Postel-Vinay, A. Varga, R. Bahleda, A. Gazzah, J.M. Michot, V. Ribrag, J.P. Armand, A. Marabelle, J.C. Soria, C. Massard, Outcomes of long-term responders to anti-programmed death 1 and anti-programmed death ligand 1 when being rechallenged with the same anti-programmed death 1 and anti-programmed death ligand 1 at progression, Eur. J. Cancer 101 (2018) 160–164.
[3] Y. Fradet, J. Bellmunt, D.J. Vaughn, J.L. Lee, L. Fong, N.J. Vogelzang, M. A. Climent, Randomized phase III KEYNOTE-045 trial of pembrolizumab versus paclitaxel, docetaxel, or vinflunine in recurrent advanced urothelial cancer: results of >2 years of follow-up, Ann. Oncol. 30 (2019) 970–997.
[4] E. Garon, M. Hellmann, N. Rizvi, E. Carcereny, Five-year overall survival for patients with advanced non–small-cell lung cancer treated with pembrolizumab: results from the phase I keynote-001 study, J. Clin. Oncol. 37 (2019) 2518.
[5] S. Gettinger, J. Choi, K. Hastings, A. Truini, I. Datar, R. Sowell, A. Wurtz, W. Dong, G. Cai, M.A. Melnick, V.Y. Du, J. Schlessinger, S.B. Goldberg, A. Chiang, M. F. Sanmamed, I. Melero, J. Agorreta, L.M. Montuenga, R. Lifton, S. Ferrone, P. Kavathas, D.L. Rimm, S.M. Kaech, K. Schalper, R.S. Herbst, K. Politi, Impaired HLA class I antigen processing and presentation as a mechanism of acquired resistance to immune checkpoint inhibitors in lung cancer, Cancer Discov. 7 (2017) 1420–1435.
[6] O. Hamid, C. Robert, A. Daud, F.S. Hodi, W.J. Hwu, R. Kefford, J.D. Wolchok, P. Hersey, R. Joseph, J.S. Weber, R. Dronca, T.C. Mitchell, A. Patnaik, H.M. Zarour, A.M. Joshua, Q. Zhao, E. Jensen, S. Ahsan, N. Ibrahim, A. Ribas, Five-year survival outcomes for patients with advanced melanoma treated with pembrolizumab in keynote-001, Ann. Oncol. 30 (2019) 582–588.
[7] J. Larkin, V. Chiarion-Sileni, R. Gonzalez, J.J. Grob, P. Rutkowski, C.D. Lao, C. L. Cowey, D. Schadendorf, J. Wagstaff, R. Dummer, P.F. Ferrucci, M. Smylie, D. Hogg, A. Hill, I. Marquez-Rodas, J. Haanen, M. Guidoboni, M. Maio, P. Schoffski, M.S. Carlino, C. Lebbe, G. McArthur, P.A. Ascierto, G.A. Daniels, G. V. Long, L. Bastholt, J.I. Rizzo, A. Balogh, A. Moshyk, F.S. Hodi, J.D. Wolchok, Five-year survival with combined nivolumab and ipilimumab in advanced melanoma, N. Engl. J. Med. 381 (2019) 1535–1546.
[8] A.V. Balar, M.D. Galsky, J.E. Rosenberg, T. Powles, D.P. Petrylak, J. Bellmunt, Y. Loriot, A. Necchi, J. Hoffman-Censits, J.L. Perez-Gracia, N.A. Dawson, M.S. van der Heijden, R. Dreicer, S. Srinivas, M.M. Retz, R.W. Joseph, A. Drakaki, U. N. Vaishampayan, S.S. Sridhar, D.I. Quinn, I. Durán, D.R. Shaffer, B.J. Eigl, P. D. Grivas, E.Y. Yu, S. Li, E.E. Kadel, Z. Boyd, R. Bourgon, P.S. Hegde, S. Mariathasan, A. Thåström, O.O. Abidoye, G.D. Fine, D.F. Bajorin, Atezolizumab as first-line treatment in cisplatin-ineligible patients with locally advanced and metastatic urothelial carcinoma: a single-arm, multicentre, phase 2 trial, Lancet 389 (2017) 67–76.
[9] T.S.K. Mok, Y.-.L. Wu, I. Kudaba, D.M. Kowalski, B.C. Cho, H.Z. Turna, G. Castro, V. Srimuninnimit, K.K. Laktionov, I. Bondarenko, K. Kubota, G.M. Lubiniecki, J. Zhang, D. Kush, G. Lopes, G. Adamchuk, M.-.J. Ahn, A. Alexandru, O. Altundag, A. Alyasova, O. Andrusenko, K. Aoe, A. Araujo, O. Aren, O. Arrieta Rodriguez, T. Ativitavas, O. Avendano, F. Barata, C.H. Barrios, C. Beato, P. Bergstrom, D. Betticher, L. Bolotina, I. Bondarenko, M. Botha, S. Buddu, C. Caglevic, A. Cardona, G. Castro, H. Castro, F. Cay Senler, C.A.S. Cerny, A. Cesas, G.-.C. Chan, J. Chang, G. Chen, X. Chen, S. Cheng, Y. Cheng, N. Cherciu, C.-.H. Chiu, B.C. Cho, S. Cicenas, D. Ciurescu, G. Cohen, M.A. Costa, P. Danchaivijitr, F. De Angelis, S. J. de Azevedo, M. Dediu, T. Deliverski, P.R.M. De Marchi, F. de The Bustamante Valles, Z. Ding, B. Doganov, L. Dreosti, R. Duarte, R. Edusma-Dy, S. Emelyanov, M. Erman, Y. Fan, L. Fein, J. Feng, D. Fenton, G. Fernandes, C. Ferreira, F. A. Franke, H. Freitas, Y. Fujisaka, H. Galindo, C. Galvez, D. Ganea, N. Gil, G. Girotto, E. Goker, T. Goksel, G. Gomez Aubin, L. Gomez Wolff, H. Griph, M. Gumus, J. Hall, G. Hart, L. Havel, J. He, Y. He, C. Hernandez Hernandez, V. Hespanhol, T. Hirashima, C.M.J. Ho, A. Horiike, Y. Hosomi, K. Hotta, M. Hou, S. H. How, T.-.C. Hsia, Y. Hu, M. Ichiki, F. Imamura, O. Ivashchuk, Y. Iwamoto, J. Jaal, J. Jassem, C. Jordaan, R.A. Juergens, D. Kaen, E. Kalinka-Warzocha, N. Karaseva, B. Karaszewska, A. Kazarnowicz, K. Kasahara, N. Katakami, T. Kato, T. Kawaguchi, J.H. Kim, K. Kishi, V. Kolek, M. Koleva, P. Kolman, L. Koubkova, R. Kowalyszyn, D. Kowalski, K. Koynov, D. Ksienski, K. Kubota, I. Kudaba, T. Kurata, G. Kuusk, L. Kuzina, I. Laczo, G.E.I. Ladrera, K. Laktionov, G. Landers, S. Lazarev, G. Lerzo, K. Lesniewski Kmak, W. Li, C.K. Liam, I. Lifirenko, O. Lipatov, X. Liu, Z. Liu, S.H. Lo, V. Lopes, K. Lopez, S. Lu, G. Martinengo, L. Mas, M. Matrosova, R. Micheva, Z. Milanova, L. Miron, T. Mok, M. Molina, S. Murakami, Y. Nakahara, T.Q. Nguyen, T. Nishimura, A. Ochsenbein, T. Ohira, R. Ohman, C. K. Ong, G. Ostoros, X. Ouyang, E. Ovchinnikova, O. Ozyilkan, L. Petruzelka, X. D. Pham, P. Picon, B. Piko, A. Poltoratsky, O. Ponomarova, P. Popelkova, G. Purkalne, S. Qin, R. Ramlau, B. Rappaport, F. Rey, E. Richardet, J. Roubec, P. Ruff, A. Rusyn, H. Saka, J. Salas, M. Sandoval, L. Santos, T. Sawa, K. Seetalarom, M. Seker, N. Seki, F. Seolwane, L. Shepherd, S. Shevnya, A.K. Shimada, Y. Shparyk, I. Sinielnikov, D. Sirbu, O. Smaletz, J.P.H. Soares, A. Sookprasert, G. Speranza, V. Srimuninnimit, V. Sriuranpong, Z. Stara, W.-.C. Su, S. Sugawara, W. Szpak, K. Takahashi, N. Takigawa, H. Tanaka, J. Tan Chun Bing, Q. Tang, P. Taranov, H. Tejada, Tho LM, Y. Torii, D. Trukhyn, M. Turdean, H. Turna, G. Ursol, J. Vanasek, M. Varela, M. Vallejo, L. Vera, A.-.P. Victorino, T. Vlasek, I. Vynnychenko, B. Wang, J. Wang, K. Wang, Y. Wu, K. Yamada, C.-.H. Yang, T. Yokoyama, T. Yokoyama, H. Yoshioka, F. Yumuk, A. Zambrano, J.J. Zarba, O. Zarubenkov, M. Zemaitis, L. Zhang, L. Zhang, X. Zhang, J. Zhao, C. Zhou, J. Zhou, Q. Zhou, A. Zippelius, Pembrolizumab versus chemotherapy for previously untreated, PD-L1-expressing, locally advanced or metastatic non-small-cell lung cancer (KEYNOTE-042): a randomised, open-label, controlled, phase 3 trial, Lancet 393 (2019) 1819–1830.
[10] R.J. Motzer, B. Escudier, D.F. McDermott, S. George, H.J. Hammers, S. Srinivas, S. S. Tykodi, J.A. Sosman, G. Procopio, E.R. Plimack, D. Castellano, T.K. Choueiri, H. Gurney, F. Donskov, P. Bono, J. Wagstaff, T.C. Gauler, T. Ueda, Y. Tomita, F. A. Schutz, C. Kollmannsberger, J. Larkin, A. Ravaud, J.S. Simon, L.A. Xu, I. M. Waxman, P. Sharma, I. CheckMate, Nivolumab versus everolimus in advanced renal-cell carcinoma, N. Engl. J. Med. 373 (2015) 1803–1813.
[11] H. Kakavand, L.A. Jackett, A.M. Menzies, T.N. Gide, M.S. Carlino, R.P.M. Saw, J. F. Thompson, J.S. Wilmott, G.V. Long, R.A. Scolyer, Negative immune checkpoint regulation by VISTA: a mechanism of acquired resistance to anti-PD-1 therapy in metastatic melanoma patients, Mod. Pathol. 30 (2017) 1666–1676.
[12] C.U. Blank, W.N. Haining, W. Held, P.G. Hogan, A. Kallies, E. Lugli, R.C. Lynn, M. Philip, A. Rao, N.P. Restifo, A. Schietinger, T.N. Schumacher, P. L. Schwartzberg, A.H. Sharpe, D.E. Speiser, E.J. Wherry, B.A. Youngblood, D. Zehn, Defining 't cell exhaustion, Nat. Rev. Immunol. 19 (2019) 665–674.
[13] B.R. Lee, S. Chae, J. Moon, M.J. Kim, H. Lee, H.W. Ko, B.C. Cho, H.S. Shim, D. Hwang, H.R. Kim, S.J Ha, Combination of PD-L1 and PVR determines sensitivity to PD-1 blockade, JCI Insight 5 (2020).
[14] R.J. Johnston, L. Comps-Agrar, J. Hackney, X. Yu, M. Huseni, Y. Yang, S. Park, V. Javinal, H. Chiu, B. Irving, D.L. Eaton, J.L. Grogan, The immunoreceptor TIGIT regulates antitumor and antiviral CD8(+) T cell effector function, Cancer Cell 26 (2014) 923–937.
[15] J.B. Lee, S.-.J. Ha, Kim HR, Clinical insights into novel immune checkpoint inhibitors, Front. Pharmacol. 12 (2021).
[16] M. Hust, T. Jostock, C. Menzel, B. Voedisch, A. Mohr, M. Brenneis, M.I. Kirsch, D. Meier, S. Dubel, Single chain fab (scFab) fragment, BMC Biotechnol. 7 (2007) 14.
[17] C. Klein, C. Sustmann, M. Thomas, K. Stubenrauch, R. Croasdale, J. Schanzer, U. Brinkmann, H. Kettenberger, J.T. Regula, W. Schaefer, Progress in overcoming the chain association issue in bispecific heterodimeric IgG antibodies, MAbs 4 (2012) 653–663.
[18] W. Zhai, X. Zhou, J. Du, Y. Gao, In vitro assay for the development of small molecule inhibitors targeting PD-1/PD-L1, Meth. Enzymol. 629 (2019) 361–381.
[19] J.H. Kim, H.J. Hong, Humanization by CDR grafting and specificity-determining residue grafting, Meth. Mol. Biol. 907 (2012) 237–245.
[20] J.D. Wolchok, H. Kluger, M.K. Callahan, M.A. Postow, N.A. Rizvi, A.M. Lesokhin, N.H. Segal, C.E. Ariyan, R.A. Gordon, K. Reed, M.M. Burke, A. Caldwell, S. A. Kronenberg, B.U. Agunwamba, X. Zhang, I. Lowy, H.D. Inzunza, W. Feely, C. E. Horak, Q. Hong, A.J. Korman, J.M. Wigginton, A. Gupta, M. Sznol, Nivolumab plus ipilimumab in advanced melanoma, N. Engl. J. Med. 369 (2013) 122–133.
[21] J. Larkin, V. Chiarion-Sileni, R. Gonzalez, J.J. Grob, C.L. Cowey, C.D. Lao, D. Schadendorf, R. Dummer, M. Smylie, P. Rutkowski, P.F. Ferrucci, A. Hill, J. Wagstaff, M.S. Carlino, J.B. Haanen, M. Maio, I. Marquez-Rodas, G.A. McArthur, P.A. Ascierto, G.V. Long, M.K. Callahan, M.A. Postow, K. Grossmann, M. Sznol, B. Dreno, L. Bastholt, A. Yang, L.M. Rollin, C. Horak, F.S. Hodi, J.D. Wolchok, Combined nivolumab and ipilimumab or monotherapy in untreated melanoma, N. Engl. J. Med. 373 (2015) 23–34.
[22] T. Yau, Y.K. Kang, T.Y. Kim, A.B. El-Khoueiry, A. Santoro, B. Sangro, I. Melero, M. Kudo, M.M. Hou, A. Matilla, F. Tovoli, J.J. Knox, A. Ruth He, B.F. El-Rayes, M. Acosta-Rivera, H.Y. Lim, J. Neely, Y. Shen, T. Wisniewski, J. Anderson, C Hsu, Efficacy and safety of nivolumab plus ipilimumab in patients with advanced hepatocellular carcinoma previously treated with sorafenib: the checkmate 040 randomized clinical trial, JAMA Oncol. 6 (2020), e204564.
[23] N.E. Ready, P.A. Ott, M.D. Hellmann, J. Zugazagoitia, C.L. Hann, F. de Braud, S. J. Antonia, P.A. Ascierto, V. Moreno, A. Atmaca, S. Salvagni, M. Taylor, A. Amin, D.R. Camidge, L. Horn, E. Calvo, A. Li, W.H. Lin, M.K. Callahan, D.R. Spigel, Nivolumab monotherapy and nivolumab plus ipilimumab in recurrent small cell lung cancer: results from the checkmate 032 randomized cohort, J. Thorac. Oncol. 15 (2020) 426–435.
[24] M.D. Hellmann, L. Paz-Ares, R. Bernabe Caro, B. Zurawski, S.W. Kim, E. Carcereny Costa, K. Park, A. Alexandru, L. Lupinacci, E. de la Mora Jimenez, H. Sakai, I. Albert, A. Vergnenegre, S. Peters, K. Syrigos, F. Barlesi, M. Reck, H. Borghaei, J. R. Brahmer, K.J. O'Byrne, W.J. Geese, P. Bhagavatheeswaran, S.K. Rabindran, R. S. Kasinathan, F.E. Nathan, S.S Ramalingam, Nivolumab plus ipilimumab in advanced non-small-cell lung cancer, N. Engl. J. Med. 381 (2019) 2020–2031.
[25] J.H. Han, M. Cai, J. Grein, S. Perera, H. Wang, M. Bigler, R. Ueda, T.W. Rosahl, E. Pinheiro, D. LaFace, W. Seghezzi, S.M.G. Williams, Effective anti-tumor response by TIGIT blockade associated with FcgammaR engagement and myeloid cell activation, Front. Immunol. 11 (2020), 573405.
[26] J. Preillon, J. Cuende, V. Rabolli, L. Garnero, M. Mercier, N. Wald, A. Pappalardo, S. Denies, D. Jamart, A.C. Michaux, R. Pirson, V. Pitard, M. Bagot, S. Prasad, E. Houthuys, M. Brouwer, R. Marillier, F. Lambolez, J.R. Marchante, F. Nyawouame, M.J. Carter, V. Baron-Bodo, A. Marie-Cardine, M. Cragg, J. Dechanet-Merville, G. Driessens, C. Hoofd, Restoration of t-cell effector function, depletion of tregs, and direct killing of tumor cells: the multiple mechanisms of action of a-TIGIT antagonist antibodies, Mol. Cancer Ther. 20 (2021) 121–131.
[27] J.D. Wolchok, V. Chiarion-Sileni, R. Gonzalez, P. Rutkowski, J.J. Grob, C.L. Cowey, C.D. Lao, J. Wagstaff, D. Schadendorf, P.F. Ferrucci, M. Smylie, R. Dummer, A. Hill, D. Hogg, J. Haanen, M.S. Carlino, O. Bechter, M. Maio, I. Marquez-Rodas, M. Guidoboni, G. McArthur, C. Lebbe, P.A. Ascierto, G.V. Long, J. Cebon, J. Sosman, M.A. Postow, M.K. Callahan, D. Walker, L. Rollin, R. Bhore, F.S. Hodi, J. Larkin, Overall survival with combined nivolumab and ipilimumab in advanced melanoma, N. Engl. J. Med. 377 (2017) 1345–1356.
[28] T. Zeng, Y. Cao, T. Jin, Y. Tian, C. Dai, F Xu, The CD112R/CD112 axis: a breakthrough in cancer immunotherapy, J. Exp. Clin. Cancer Res. 40 (2021) 285.
[29] S. Whelan, E. Ophir, M.F. Kotturi, O. Levy, S. Ganguly, L. Leung, I. Vaknin, S. Kumar, L. Dassa, K. Hansen, D. Bernados, B. Murter, A. Soni, J.M. Taube, A. N. Fader, T.L. Wang, I.M. Shih, M. White, D.M. Pardoll, S.C. Liang, PVRIG and

PVRL2 are induced in cancer and inhibit CD8(+) t-cell function, Cancer Immunol. Res. 7 (2019) 257–268.